

NASA Technical Paper 1149

NASA Ground-Based and Space-Based Laser Ranging Systems

Michael W. Fitzmaurice

JANUARY 1978

NASA

NASA Technical Paper 1149

NASA Ground-Based and Space-Based Laser Ranging Systems

Michael W. Fitzmaurice
Goddard Space Flight Center
Greenbelt, Maryland



National Aeronautics
and Space Administration

**Scientific and Technical
Information Office**

1978

This document makes use of international metric units according to the Systeme International d'Unites (SI). In certain cases, utility requires the retention of other systems of units in addition to the SI units. The conventional units stated in parentheses following the computed SI equivalents are the basis of the measurements and calculations reported.

CONTENTS

	<i>Page</i>
INTRODUCTION AND SCOPE	1
APPLICATIONS AND SYSTEM EVOLUTION	2
CURRENT STATE OF THE ART	8
PLANS FOR SHUTTLE-BASED LASER RANGING SYSTEMS	18
CONCLUSIONS	22
ACKNOWLEDGMENTS	22
REFERENCES	23

NASA GROUND-BASED AND SPACE-BASED LASER RANGING SYSTEMS *

Michael W. Fitzmaurice
*Goddard Space Flight Center
Greenbelt, Maryland*

INTRODUCTION AND SCOPE

The development of laser ranging systems within the National Aeronautics and Space Administration (NASA) started in the early 1960's, soon after the invention of the laser. This program has grown substantially in the intervening years, and has produced important results in the areas of precision-orbit determination and gravity-field determination. In addition, laser ranging is expected in the near future to produce some unique results on crustal motions of the Earth. These results may be very important for understanding the mechanisms which cause earthquakes.

This document presents an overview of the NASA laser ranging program. The discussion covers the following:

- Applications and system evolution (1962-1976)
- Current state of the art
 - Performance
 - Hardware
 - Error sources
- Plans for Shuttle-based laser ranging systems

The principal applications that these systems address are outlined, and the characteristics of typical systems built during the 1960's and early 1970's are described. The current state of the art, as exemplified by some of the more recent ranging systems, is also discussed with respect to performance levels and to error sources which limit this performance. The final section discusses NASA plans for using laser ranging systems aboard the Space Shuttle.

*Presented as an invited paper at the Conference on Laser Engineering and Applications (CLEA) in Washington, D.C., June 1-3, 1977.

APPLICATIONS AND SYSTEM EVOLUTION

In principle, many types of laser systems could be used for ranging to satellites. The type discussed here, which is the most widely used approach, is shown functionally in figure 1.

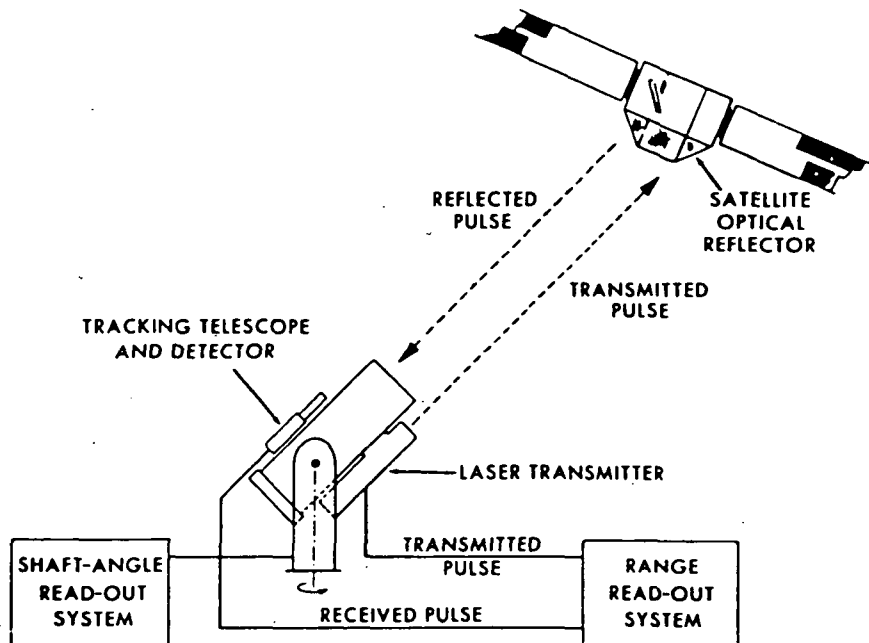


Figure 1. Laser satellite tracking experiment.

A pulsed laser transmitter and receiver are boresighted and mounted on a two-axis gimbal system. The pointing direction is read out by shaft encoders, and the pointing direction is controlled either manually or by a computer using orbit predictions. A portion of the outgoing pulse is picked off and used to start a time-interval unit. Because the satellite is equipped with optical cube corners on its Earth-viewing side, the incident pulse is reflected back on itself and is detected at the receiver. This received pulse terminates the time-interval measurement. The time of flight is stored, and the entire process is repeated at a 1-pps rate.

This type of system has been applied to several measurement problems; some of the more important are:

- Orbit determination
- Polar motion
- Gravity field studies

- Earth tides
- Tectonic-plate motion

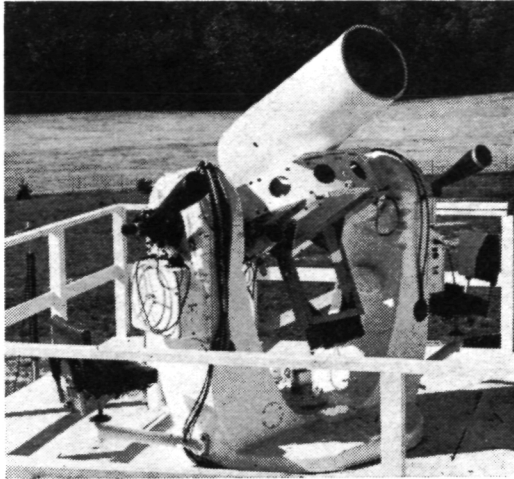
By using the accurate range measurements and information on the orbit plane, which can be obtained from the shaft encoders or the coarse orbit predictions, the orbit can be determined to meter accuracy. The orbit will change with time because of the various forces that act on the spacecraft; the largest of these forces is the gravity field. By measuring orbit changes with time, the magnitude of the various spatial frequencies in the geopotential field can be evaluated (Reference 1).

It is generally accepted that the Earth's polar axis changes position very slowly, about $1/5^\circ$ per million years. In addition, short-term variations occur in pole position that are believed to be correlated with earthquakes (Reference 2), and it is these motions that a satellite laser ranging system can monitor. The basic measurement is to determine any shifts in the apparent orbital inclination of the satellite (Reference 3). Because the true orbit inclination in inertial space is very well determined, a short-term anomalous shift can be attributed to a shift in the latitude of the ground station, which is, in effect, caused by a shift in the location of Earth's polar axis.

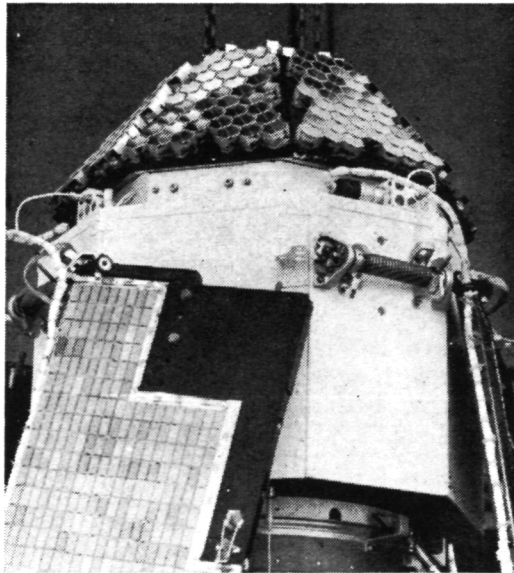
In addition to the ocean tides, there are significant but poorly understood solid Earth tides (Reference 4). These deformations affect the "G" field that an orbiting satellite sees, and, by measuring the resulting orbit perturbations, the magnitude of the Earth tide can be inferred, and the elastic properties of the Earth's interior can be estimated. This is potentially important for resources assessment, such as the locating of mineral and oil deposits.

Within the geophysics community, it is now generally accepted that the surface of the Earth is composed of about a dozen or more plates that are essentially floating on a fluid-like core. The boundaries of these plates are known to be relatively high-risk earthquake regions, but the actual magnitude of the risk depends on the differential motion of adjoining plates. Such differential motions are now being measured for the first time by laser ranging systems, and this particular application (tectonic-plate motion) is currently the single most important use of satellite laser ranging. The focus for this activity is the San Andreas Fault Experiment (SAFE) (Reference 5). The details of this experiment will be discussed in the following section.

The first satellite laser ranging took place in 1964 (Reference 6) with the hardware shown in figure 2. The laser transmitter and the receiver were mounted on a platform inside the two axes of this Nike-Ajax mount. Acquisition was accomplished by using orbital predictions from the Minitrack network; the satellite was then tracked visually by two operators who controlled the azimuth and elevation axes. Tracking was possible only at night during that portion of the pass in which the Sun illuminated the satellite. The laser was a mechanically Q-switched ruby that supplied about 800 mJ into a 1.2-mr beamwidth. The receiver phototube was mounted at the prime focus of the 16-inch telescope, and the start and stop signals were cabled to instrumentation below the platform.



(a) Transmitting laser and receiving telescope mounted on a modified Nike-Ajax radar pedestal



(b) Beacon Explorer-B Satellite with array of cube-corner reflectors

Figure 2. Satellite laser ranging (1964).

The satellite was called Beacon Explorer-B, although its formal name was Explorer-22. It was magnetically stabilized with its north-seeking end studded with optical cube corners. The satellite was inserted into a 980-km near-polar orbit in October 1964, and, within 3 weeks, it was being tracked by this system. Laser tracking was possible only in the northern hemisphere because of the satellite's magnetic stabilization.

Because of the high tangential velocity between the ground station and the target, the signal reflected from the satellite does not come precisely back to the ground station, but instead is offset angularly by about 10 arc-seconds. Therefore, if the cube corners produced a diffraction-limited return beam, the footprint of the return signal would not cover the ground station. To accommodate this effect (called the velocity aberration or Bradley effect), the cube corners were designed to produce a 20-arc-second reflected beamwidth.

Although 13 years old, this particular satellite continues to serve as an excellent target for laser ranging systems.

After about 1 year of tracking from this station, it became obvious that the usefulness of this system would be much improved if it were mobile. Figure 3 shows the concept that evolved.

The pointing system is now an integral part of a trailer that can be towed by a standard tractor. The laser is no longer mounted on the pointing platform but is now located on a fixed optical bench within the trailer. The output beam is directed up to the pointing platform by a series of flat mirrors, is collimated by a small telescope, and is transmitted to the satellite. This approach has several advantages: It simplifies the thermal and electrical interface to the laser because it is no longer necessary for liquid cooling loops and electrical power cabling to cross the gimbals, and it increases the stability and reliability of the laser because it operates in a temperature-controlled and stationary environment.

After being set up on a concrete pad, the mount and laser bench are isolated from the trailer structure and are supported directly from the pad by attaching legs. The receiver is mounted at the prime focus of the large telescope.

In this first-generation system, all the instrumentation for the operation is located in a single van, including the laser system, the receiver electronics, the computer, and the control electronics for the mount and the data storage system. In follow-on systems, the receiver and computer systems were put in a separate van to reduce radio frequency (RF) interference problems associated with laser firing and to simply provide more space.

An RF radar is also required for safety purposes. The laser system is shut down when an aircraft is detected within 20° of the laser-pointing direction. A minimum of three people are needed during satellite tracking: a safety observer, a mount operator, and a console operator.

Figure 4 shows the Moblas-II system that was built at the Goddard Space Flight Center (GSFC) in the late 1960's. The mount is equipped with 22 bit encoders. A ruby laser that operates

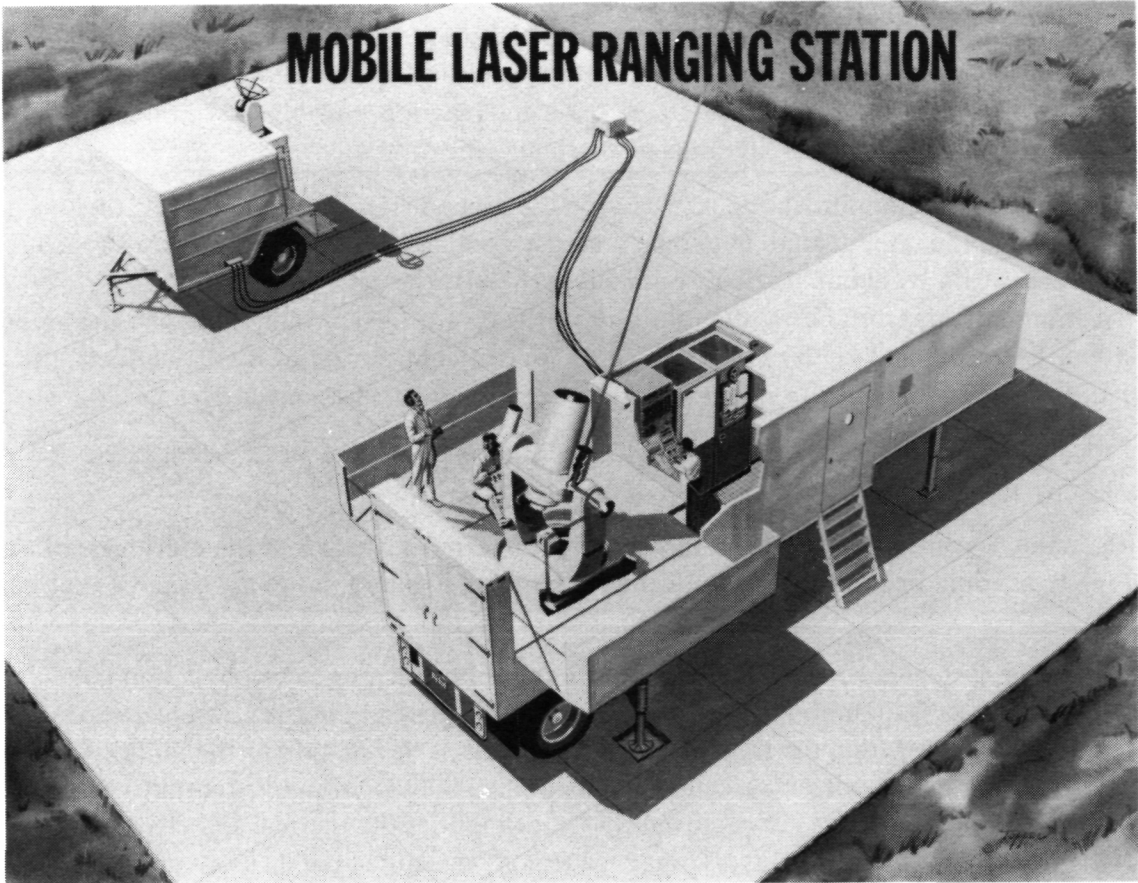


Figure 3. Mobile laser ranging station.

in the cavity dump mode is located in the van and produces a 5-ns pulse with about 1/4 joule of energy. The beam enters the base of the mount and is directed up through the light pipe and then out through a 5-power collimator. The exiting beam divergence is about 40 arc-seconds. Experience has shown that it normally takes about 2 weeks on site to complete the setup and to start satellite tracking. At the end of the tracking period, which is typically a couple of months, it takes about 1 week to disassemble the system for moving to the next location.

The Moblas-III laser system was built at GSFC in 1976. This system has two vans: one for the laser and pointing system (shown in figure 5) and one van for the computer and receiver signal processor. As in Moblas-II, the laser is at a fixed-coudé focus but, in this case, is transmitted through a 20-cm collimating telescope.

Figure 6 shows the signal flow for a typical ranging system. A time standard with a 1-pps output signal furnishes the trigger for the laser. About 1 millisecond or so later, the laser pulse exits the transmitter. A small portion of this pulse is picked off by a photodiode and put into a threshold detector. The output of this unit starts the time-of-flight measurement.



Figure 4. Moblas-II system.

This output also permits measurement of the elapsed time between the laser trigger pulse and the actual time at which emission occurs. The transmitted waveform is also recorded so that the amplitude-dependent time-walk in the threshold detector can be accounted for.

The return signal from the satellite is detected by a photomultiplier. The output of this tube is leading-edge detected and is used to stop the time-interval unit. This discriminated signal is also used to trigger a waveform digitizer that stores the received pulse shape. The range time-interval unit then supplies the coarse time-of-flight information, and the two waveforms (transmitted and received) are analyzed to obtain the vernier correction.

The data input to the computer then includes the time-interval unit value, the two waveforms, and the time of day at which the measurement was made. When two or more ground stations are acquiring data on the same satellite, their respective clocks must be synchronized to $5 \mu\text{s}$ or better.

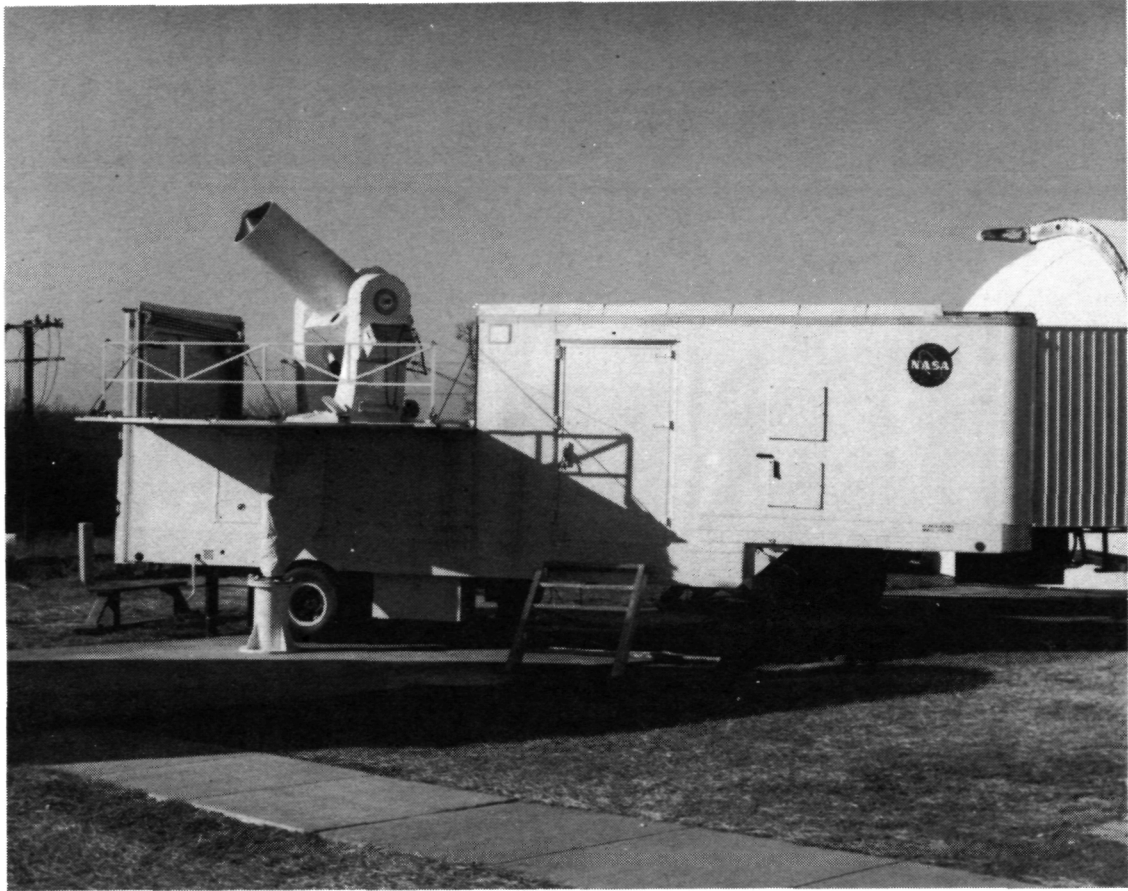


Figure 5. Moblas-III laser system.

CURRENT STATE OF THE ART

Figure 7 summarizes the performance improvement of satellite laser ranging systems over the last 12 to 13 years. As previously mentioned, the first tracking occurred in October 1964. This was a nighttime operation only because the orbital predictions were not accurate enough to permit open-loop pointing with milliradian beamwidths. As the laser data came in, both orbits and gravity-field models were refined, and, by 1968, it was possible to track both day and night.

The initial precision connected with the orbit determination was a few meters. The bottom curve (figure 7) represents the best system performance, whereas the upper curve is more of an average or typical value. The precision increased dramatically in the late 1960's and early 1970's because of improvements in transmitters, receivers, and signal processing.

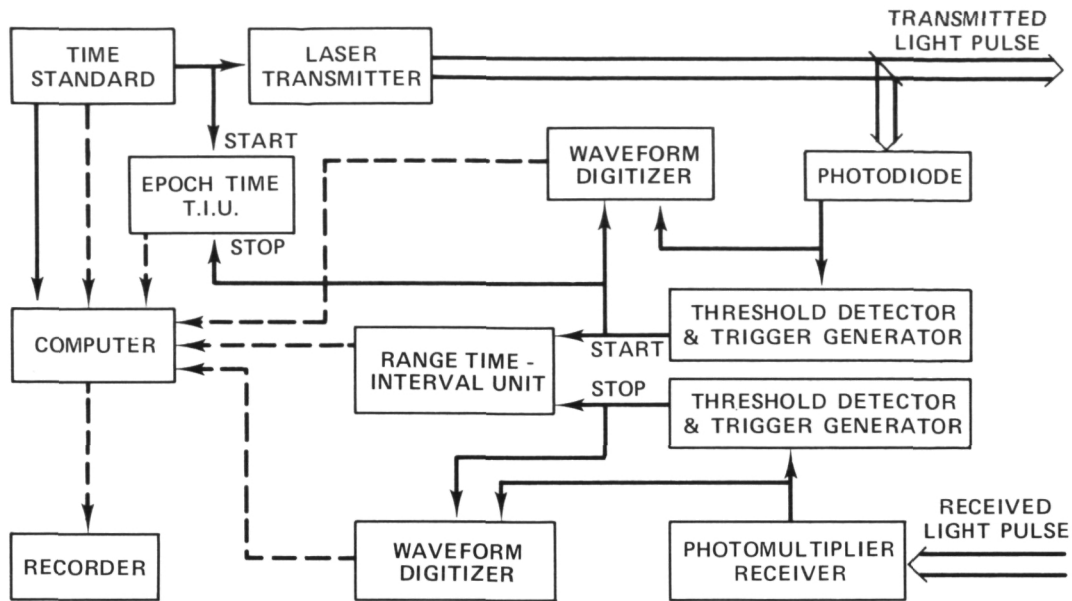


Figure 6. Laser ranging system.

The early transmitters were mechanically Q-switched lasers with pulse widths of about 25 to 50 ns. In the early 1970's, these were upgraded with electro-optic Q-switches and external pulse slicers to achieve 5 to 10 ns. Most of the systems are now operating with cavity-dump lasers that provide a 4- to 5-ns pulse width.

The early receivers used leading-edge detection; that is, a fixed-threshold detector. Later, the amplitude of the return pulse was recorded and used to correct the time-walk characteristics of the discriminator. The entire received waveform is now recorded, and centroid or cross-correlation detection is used to establish time of arrival.

The launch dates for the various satellites that have laser reflectors are shown at the bottom of figure 7. The first, Explorer-22, was launched in October 1964, and the last Laser Geodetic Earth-Orbiting Satellite (LAGEOS), was launched in May 1976. Two more satellites are scheduled for launch in 1977 and 1978.

Table 1 lists the various laser ranging satellites that are now in orbit. They are listed chronologically according to launch date. There are currently seven U.S. satellites and four French; two more are planned for 1977 and 1978. In general, these satellites carry several instruments; the laser reflectors are merely one of the instruments. The exceptions are Lageos and Starlette, which are devoted exclusively to laser ranging.

The altitude of most of the satellites is 1000 km, except for NTS-I (a Naval Research Laboratory mission) and Lageos, which are significantly higher. Although the low orbits make the radar link less difficult, they reduce the visibility time per pass and, in addition, cause problems in data analysis because the errors in gravity-field models and atmospheric-drag models are greater for low orbits.

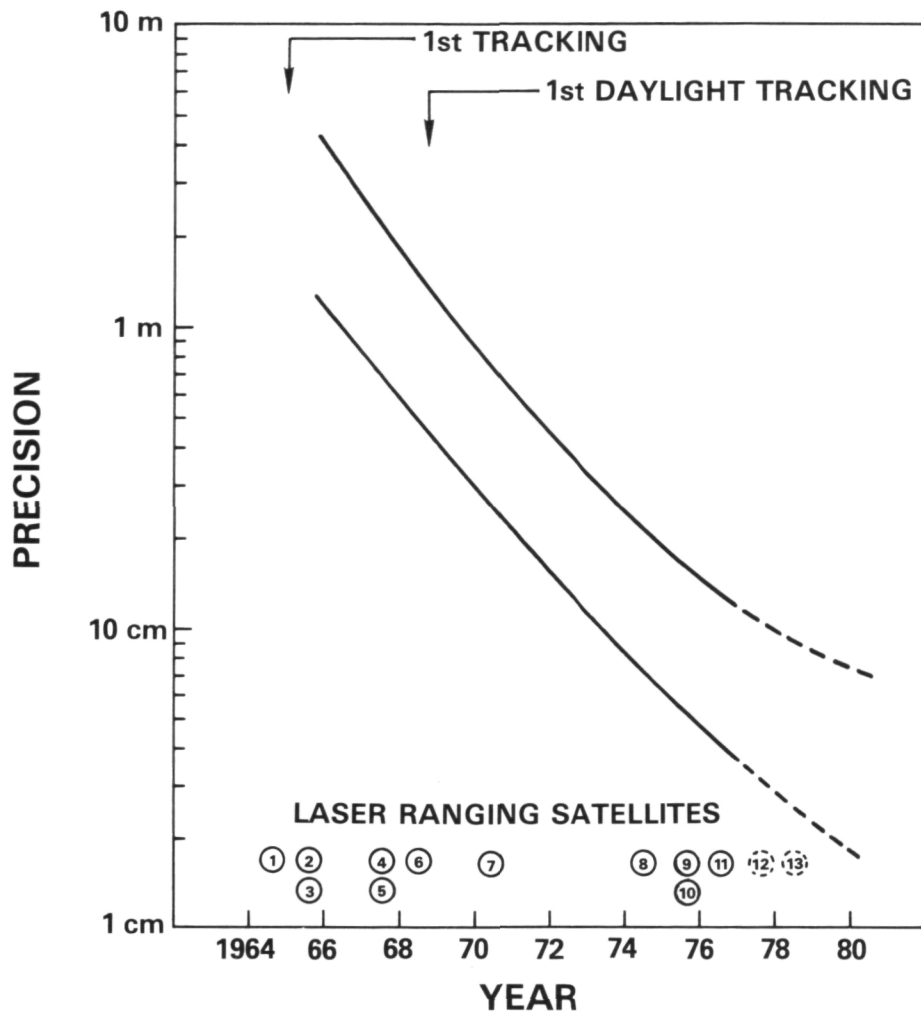


Figure 7. Evolution of satellite laser ranging system performance.

The optical-radar cross section (table 1) is listed in millions of square meters. These numbers appear to be extremely large because of the very small divergence on the reflected beam. Typically, a 1-inch near-diffraction limited cube corner has a cross section of about 1 million square meters.

The cross section and range enter the radar equation in this way (σ/R^4); this ratio therefore gives a quick indication of the level of difficulty in tracking the various satellites. These values are tabulated for the zenith condition and for the more typical 45° elevation case. The ratio spans four orders of magnitude. Because most systems are designed to be able to track Lageos, they will operate with a very high average photoelectron level for most of the other satellites.

Table 1
Laser Ranging Satellites

Satellite	Altitude $m \times 10^6$	Zenith Cross Section $m^2 \times 10^6$	Cross Section \div (Slant Range) ⁴	
			Zenith	45°
Explorer-22 (US) BE-B	0.98	5.4	5.4	1.8
Explorer-27 (US) BE-C	1.1	5.0	3.2	0.99
Explorer-29 (US) GEOS-I	1.7	57.0	6.8	0.24
Diadem-I (FR)	0.94	3.8	4.9	1.3
Diadem-II (FR)	1.2	3.8	1.7	0.58
Explorer-36 (US) GEOS-II	1.3	100.0	32.0	1.2
Peole (FR)	0.60	0.80	6.2	4.2
NTS-I (US)	14.0	103.0	0.0030	0.0011
Starlett (FR)*	0.96	0.65	0.76	0.22
GEOS-III (US)	0.90	1.9	2.9	18.00
Lageos (US)*	5.9	7.0	0.0057	0.0018
NTS-II (US)	20.0	252.0	0.0015	0.00064
Seasat-A (US)	0.85	3.8	7.3	6.8

*Dedicated.

Table 2 lists the stations that make up the NASA laser tracking network. Three are mobile stations and five are fixed location stations. The Smithsonian Astrophysical Observatory (SAO) operates four stations for NASA. Five more mobile stations are being built and will begin to become operational in 1978.

The stationary laser (Stalas) is a frequency-doubled Nd:YAG; the other systems use ruby lasers and amplifiers. The new mobile systems will use frequency-doubled Nd:YAG. The receiver apertures are from 0.41 m (16 inches) up to 0.76 m (30 inches). At least two figures of merit can be used to describe a laser ranging system; the first, M_T , defined as $E_t D_r^2 / \theta_t^2$, scales the number of photoelectrons received per pulse and is therefore a key parameter in determining target-miss probability. The second, M_r , as defined as $M_T^{1/2}$ / pulse width, is directly proportional to the accuracy with which the arrival time of a low-level optical pulse can be estimated. These calculations indicate that Stalas should have the highest performance capabilities, and comparison of satellite tracking data indicates that this is, in fact, the case.

Table 2
Laser Ranging Stations

Station	Location	E_t (Joules)	D_r (Meters)	M_T^* $J\text{-m}^2 \times 10^6$	M_R^\dagger $J^{1/2}\text{-m/s} \times 10^{11}$
Moblas-I	Mobile	1.0	0.41	4.2	4.1
Moblas-II	Mobile	0.25	0.51	1.6	2.5
Moblas-III	Mobile	1.0	0.51	6.5	5.1
Stalas	Maryland	0.25	0.51	6.5	51.0
SAO-I	Brazil	6.0	0.51	0.25	0.2
SAO-II	Peru	6.0	0.51	0.25	0.2
SAO-III	Australia	6.0	0.51	0.25	0.2
SAO-IV	Arizona	6.0	0.51	0.25	0.2
Moblas-IV, -V, -VI, -VII, and -VIII	Mobile	0.25	0.76	14.0	7.5

*Tracking figure of merit, $M_T = E_t D_r^2 / \theta_t^2$.

†Ranging figure of merit, $M_R = (M_T)^{1/2} / \text{pulse width}$.

A number of factors limit the performance of the current systems. The principal error sources are:

- Atmospheric delay
 - 2.5- to 10-meter correction
 - Models appear valid ≤ 1 cm
 - $\delta R / \delta P = 0.5$ cm/MB, $\delta R / \delta T = 0.01$ cm/K, $\delta R / \delta \epsilon = 0.01$ cm/%RH
- Optical signal-to-noise ratio
 - $\sigma \sim \text{pulse width} / (\text{average photoelectrons})^{1/2}$
- Electron multiplier
 - Photoemission with varying \bar{V}
 - Electron optics
- Time-interval measurement
 - Commercial units ~ 1.5 cm
 - Developmental unit ~ 0.1 cm

- Target noise
 - Coherent fading, pulse distortion
 - Center-of-gravity correction

Because the propagation velocity of an optical pulse through air is a few parts in 10^4 smaller than the free-space value, the measured range to the satellite based on transit time is somewhat longer than the true geometric range. This effect amounts to about 2.5 meters at zenith and approaches 10 meters at 10° elevation. Several models have been developed for predicting the atmospheric corrections. The Marini/Murray algorithm (Reference 7) is used in the GSFC systems. This model was recently checked by Gardner at the University of Illinois, using sets of simultaneous radiosonde data (Reference 8), and it appears to be accurate to approximately 1 cm at elevation angles down to 20° . As input, the model requires the pressure, temperature, and relative humidity at the ground station. The accuracies of these meteorological inputs are important, particularly the pressure data. The error sensitivities are listed with the error sources given previously. The pressure input is the most critical.

A calculation of the maximum likelihood estimator for the arrival time of an optical pulse shows that the standard deviation varies as (pulse width) \times (average photoelectrons per pulse) $^{-1/2}$ (Reference 9). For pulse widths in excess of a few nanoseconds, this becomes an important consideration. Typically, if ranging is performed with a 5-ns pulse (full width at half-maximum (FWHM)) and 5-cm precision is desired, an average signal level of about 6 photoelectrons per pulse is required. This is the theoretical limit; a more reasonable operating level would be about two to three times this amount.

The electron multiplier in the photomultiplier introduces timing noise caused by the varying transit times that electrons experience as they travel from photocathode to anode. The best electrostatic tubes have a transit-time jitter of about 300 ps for single photoelectrons (Reference 10). This is significant because it maps into a 4.5-cm ranging error. Some recent measurements on static crossed-field photomultiplier tubes indicate that their jitter is about an order of magnitude less than this (Reference 11); this problem should therefore become less important in the future.

Another error source is the time-interval measurement. The question is simply this: How accurately can the time interval between a pair of pulses that have a nominal separation of 5 to 10 milliseconds be measured? The best commercial units have about 100-ps accuracy, which maps into a 1.5-cm ranging error (Reference 12). A unit recently developed at Lawrence Berkeley Laboratories has a measured accuracy of about 10 ps (Reference 13), so that this error source should also become less important in the future.

The satellite itself is another important error source. There are two noise mechanisms at work in this case (Reference 14). First, because several cube corners contribute to the return signal, coherent fading occurs in the far field at the receiver. The return pulse is broadened, but, more importantly, it is distorted in a random fashion. Another noise source is called the center-of-gravity correction. When ranging to a satellite, it is desired to measure the

range from the ground station to the center of gravity of the satellite because it is the satellite center of gravity whose path can be predicted as it travels through the gravity field. Because actual measurement is to cube-corners on the surface of the satellite, some correction must be applied to this related to the center of gravity. The last satellite that was launched, Lageos, was designed specifically to minimize both these noise sources.

Figure 8 shows Lageos during prelaunch testing at GSFC. It is a small heavy sphere (411 kg, 60-cm diameter) and is studded with 426 optical-cube corners. Serving as a laser ranging target, this satellite introduces very little pulse-spreading because only reflectors that are aligned with the incident pulse to about $\pm 10^\circ$ participate in the return signal. For any orientation, only about eight to ten reflectors contribute significantly to the return.

Figure 9 shows both the results of the prelaunch testing and the test laboratory (Reference 15). The average pulse-spreading was about 125 ps; the effective reflection surface is about 5 cm beneath the skin of the satellite, but, more importantly, the radius of the reflection surface varies with attitude by only about 2 mm.



Figure 8. Lageos during prelaunch testing at GSFC.

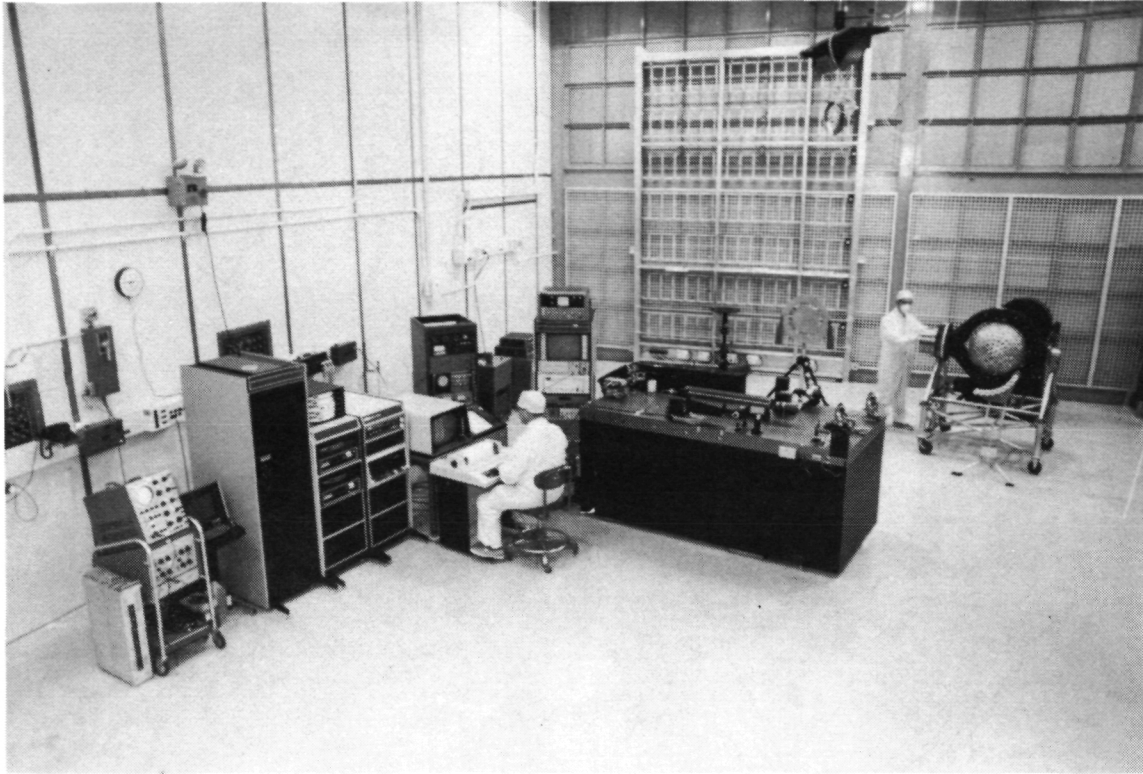


Figure 9. Lageos test laboratory.

Lageos was launched in May 1976 from the Western Test Range and was tracked shortly thereafter by SAO ground stations and the GSFC Stalas system. One of the more successful Stalas tracks is shown in figure 10. The satellite was acquired by Stalas at an elevation angle of about 54° and was tracked continuously for about 30 minutes down to an elevation angle of about 23° . The data for this pass are summarized in figure 11.

The ranging system operated at a 1-pps rate so that, in 30 minutes, about 1800 pulses were transmitted. Of these, 805 returns were strong enough to exceed the preset receiver threshold level. These ranging measurements were adjusted for atmospheric refractivity using the Marini-Murray algorithm, and a best-fit orbit was generated for the pass using a high-order polynomial. The residuals (i.e., the difference between the measurements and the best fit orbit) are plotted in figure 11. The root-mean-square value of the residuals is 4.5 cm.

These data are representative of the state of the art in satellite laser ranging today. Unfortunately, this particular data set is not typical, but it should be regarded as one of the better data sets. However, it is typical of the achievement expected as the ground stations are upgraded.



Figure 10. Lagoons tracked by GSFC, June 27, 1976.

This capability for measuring ground-to-satellite distances to an accuracy of a few centimeters has been used to study several geophysical phenomena, as discussed in the section on “Applications and System Evolution,” but the most exciting application at this time is the measurement of tectonic-plate motions. In most cases, the boundaries of these plates are well defined, and the plates are moving at rates of about 1 to 10 cm per year with respect to one another.

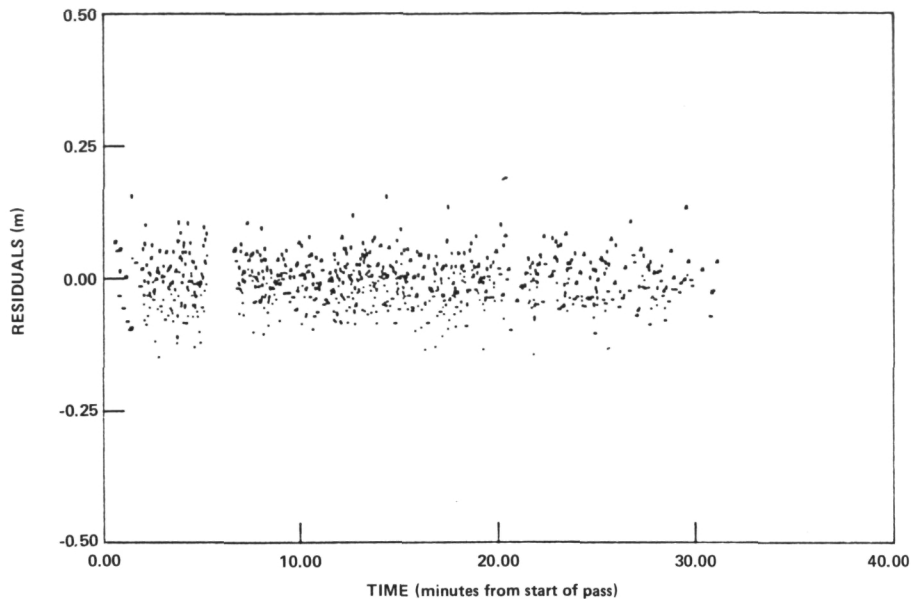


Figure 11. Stalos range residuals versus time for Lageos.

Because comparison of a map of earthquake occurrences with a map that outlines plate boundaries shows a very high correlation, it is clear that areas close to plate boundaries are potentially high-risk areas for earthquakes. The magnitude of the risk for a particular area depends on the rates at which the plates are moving with respect to one another and on whether the local plate boundaries are slipping smoothly or locked together. Up to this time, there has been no direct measurement of plate motion; the only measurements are based on paleomagnetic results that have an averaging time of about 50 million years.

The San Andreas Fault Experiment (SAFE), now in the middle of a 10-year experiment to make the first relatively short-term plate motion measurements, is outlined in figure 12. The San Andreas Fault separates the Pacific and American Plates. These plates are thought to be moving with respect to one another as shown in the slide. Laser ground stations have been located at San Diego and Quincy, California, and Bear Lake, Utah, and are eventually planned for two locations in Mexico.

The laser stations range to a satellite as it passes over and use the data to both define the orbit and determine their relative locations. Independent baseline determinations will be made every 2 years, with changes in these baselines indicating what the plate motion rates are.

The experiment began in 1972 when Quincy and San Diego were occupied for about 2 months. It was repeated in 1974 at the same locations and repeated in 1976 with Bear Lake included. All three locations will be occupied again in 1978.

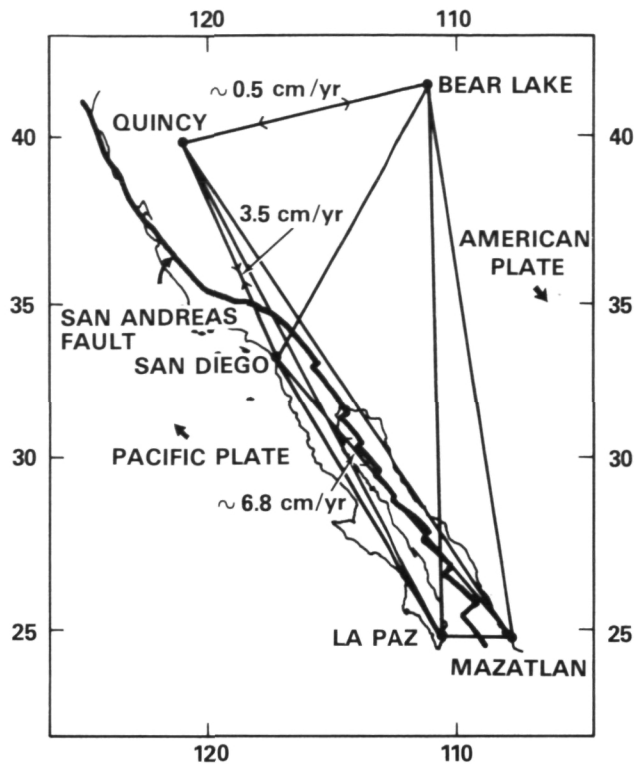


Figure 12. Proposed site locations for the San Andreas Fault Experiment.

The SAFE results to date for the San Diego/Quincy baseline are:

- Simulations—predict precision of 2 cm by 1980
- Measurements
 - 1972 data—896275.92 m, $\sigma = 10$ cm
 - 1974 data—896275.83 m, $\sigma = 7$ cm
 - 1976 data—now being reduced

Detailed simulation studies included error sources such as gravity field, atmospheric drag, solar pressure, and laser-system measurement noise (Reference 16). The results of these simulations indicate that the baselines should be recoverable to 2 cm by 1980. The baselines determined from the laser measurements are at the bottom of the chart for the 1972 and 1974 data. The baselines differ by 9 cm, but, because of the 10- and 7-cm noise levels, it is too early to draw conclusions. It does appear, however, that results comparable to those predicted by the simulations will be achieved by 1980.

PLANS FOR SHUTTLE-BASED LASER RANGING SYSTEMS

In addition to measuring the macroscopic aspect of tectonic-plate motion, there is clear need for measuring crustal deformations on a much smaller spatial scale so that earthquake

precursors such as dilatency can be detected. To cover an area such as California, several hundred (perhaps thousands) ground points must be repetitively surveyed.

The mobile laser ranging stations described earlier can be relocated at a maximum of about 5 to 10 different points per year. Therefore, even if a dozen or more of these stations were available, it is doubtful that they could cover the needed number of ground points.

As an alternate approach to this problem, it was suggested some time ago that the laser ranging system be turned "upside down" (Reference 17). In this case, a single laser transmitter/receiver is installed on a spaceborne platform, and low-cost passive ground targets are located at all points of interest. This approach, which has been under development at GSFC for several years, is shown conceptually in figure 13 in which the spaceborne platform is provided by the Space Shuttle (References 18 and 19). The laser is pointed at a particular target for a short period of time and obtains range measurements. The laser is then pointed to adjacent targets in a sequential manner and obtains range measurements to each. These measurements are used: (1) to define the Shuttle orbit during the measuring period, and (2) using trilateration, to measure the relative positions of the ground targets.

Figure 14 shows the operational scenario. The laser system initiates the measurement sequence when it is at a 20° elevation (as seen from the first ground target). The system transmits at a 10-pps rate for about 2.5 seconds, thereby obtaining 25 range measurements. The laser is then pointed to the next target and repeats the sequence. To provide a strong geometrical solution it is planned to survey the entire grid three times during a single Shuttle pass.

The first map will be at low elevation angles at the beginning of the pass, the second map, at high elevation angles (near zenith), and the final map, at low elevation angles near the end of the pass. The current plan is to fly this system on a series of Shuttle flights in the 1981–1983 time frame. The purpose of these flights is two-fold: (1) to demonstrate and validate the measurement technique, and (2) to obtain the first broad-coverage strain-accumulation data for the Southern California area.

Figure 15 shows the planned ground network, which includes a total of 42 ground targets spaced at intervals that vary from 25 to 100 km. This network contains a ground-truth area consisting of a cluster of targets spaced at 25-km intervals. These particular targets will be surveyed-in before the first flight using first-order techniques to permit a determination of their relative location to about 2 cm. These data will be compared to the laser-derived data after the first mission to establish the validity of the space-based technique.

A total of five Shuttle missions are planned. On each mission, the relative locations of all targets in the network will be established with a precision of a few centimeters. Subsequent flights will remeasure the grid since changes in the relative positions are expected because of crustal motions. These changes in relative position produce a strain-accumulation pattern, and the accompanying stress pattern will permit an assessment of the earthquake risk level throughout the region. Such measurements are not possible with ground-based instrumentation because of line-of-sight limitations.

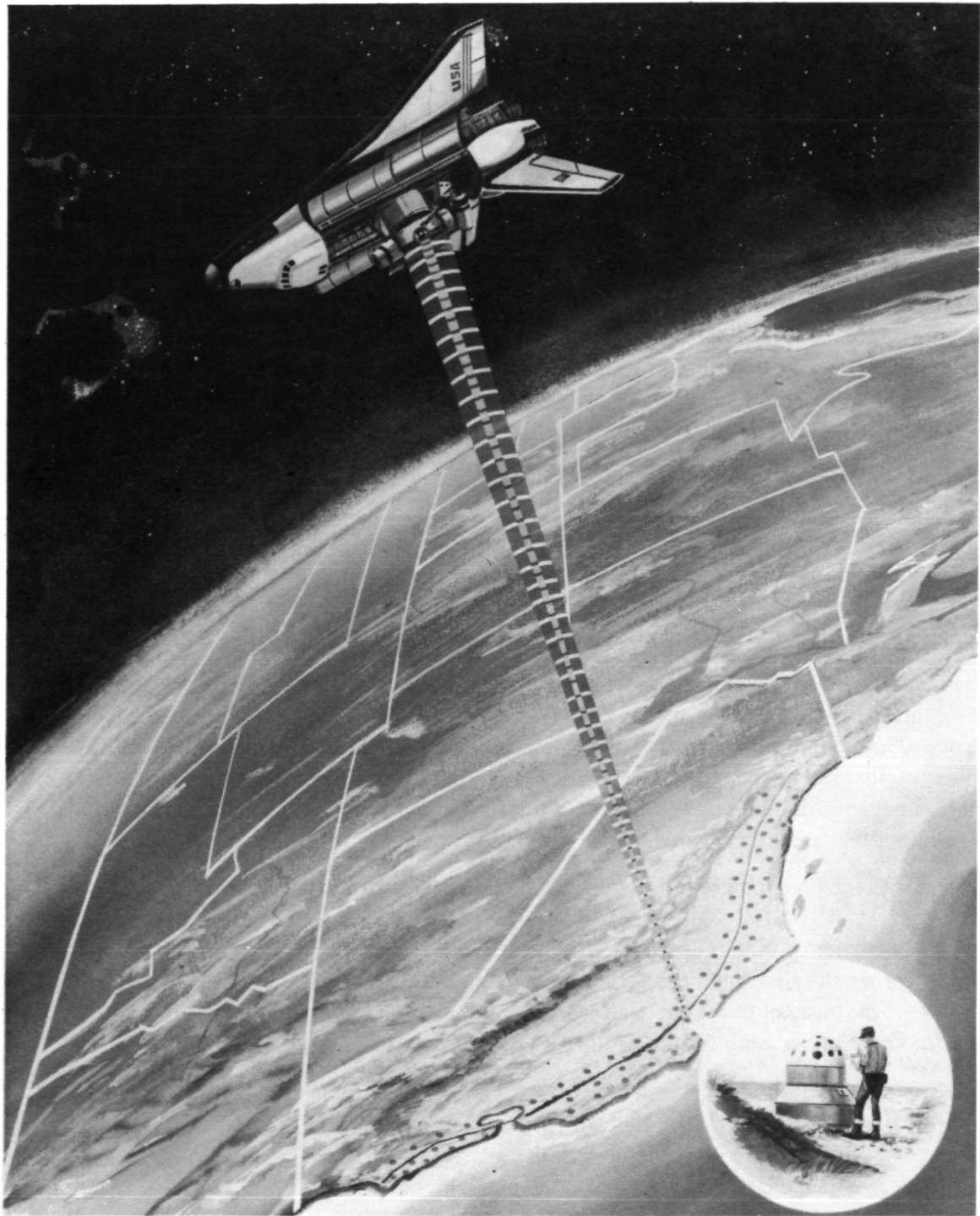


Figure 13. Artist's conception of laser ranging system operating upside down from spaceborne platform.

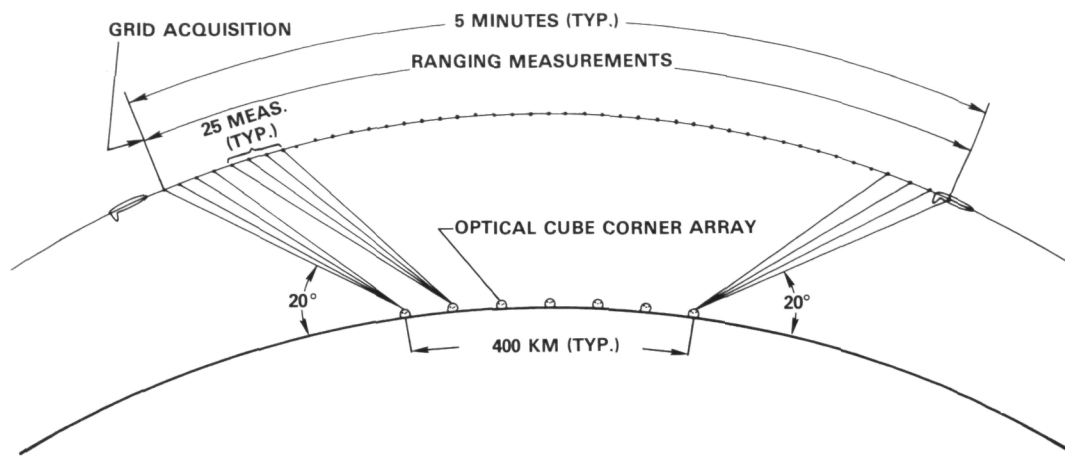


Figure 14. Shuttle-based laser ranging system.

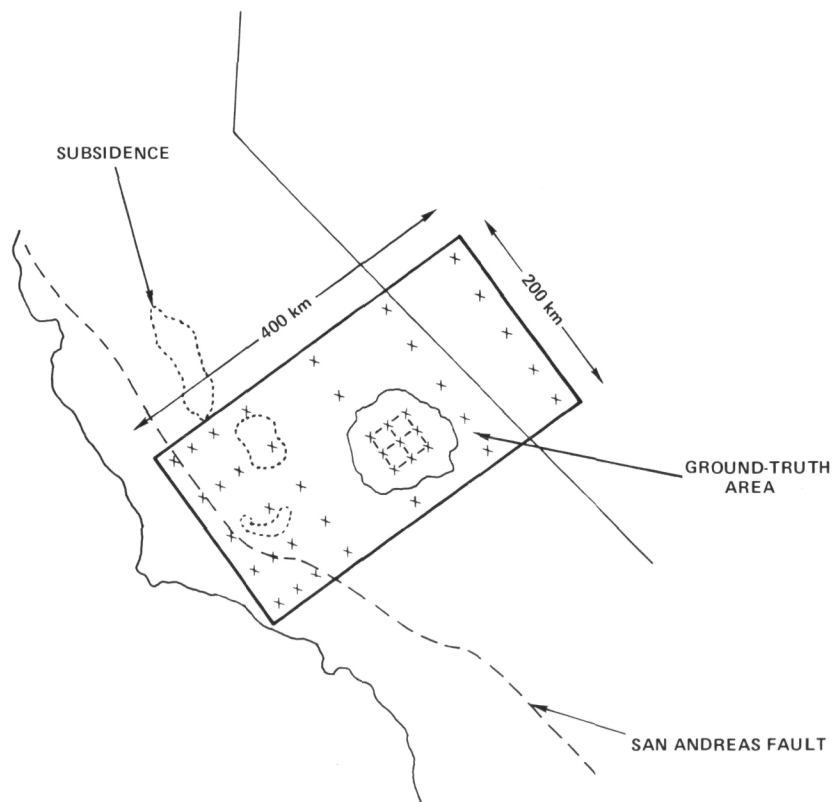


Figure 15. Experiment network in the California-Nevada area.

Extensive digital computer simulations have been performed for this system, and the results of a typical simulation are:

- Assumptions

Laser system	10-cm noise, 0.3-cm bias
Pulse rate	10 pps
Clear skies over experiment area	25 percent
Air-drag error	20 percent
Solar-radiation pressure error	33 percent
Earth-mass error	5×10^{-7}
Gravity-model error	GEM-6 error statistics
- Ground network—Five corner-cube arrays in cross formation, 50 km apart
- Results—Relative positions of arrays recovered to ± 2 cm, both horizontally and vertically

As these results indicate, the relative locations of the targets can be recovered in three dimensions with a standard deviation of about 2 cm. In this case, the ground network consisted of only five targets. Results of more recent simulations using the full complement of 42 targets are essentially the same.

CONCLUSIONS

In conclusion, it appears that the deployment of a laser ranging system on a space platform offers the opportunity to perform a unique set of measurements that may be very important to the development of predictive models for earthquakes. There is a very strong interest within NASA for the development and flight testing of a prototype system for this purpose.

ACKNOWLEDGMENTS

The work summarized in this document was performed by a large number of groups from industry, academia, and government over the last 17 years. The author will not attempt to acknowledge all the individual groups, but it is appropriate to note the pioneering contributions of the laser ranging teams at the Goddard Space Flight Center and the Smithsonian Astrophysical Observatory.

Goddard Space Flight Center
National Aeronautics and Space Administration
Greenbelt, Maryland November 1977

REFERENCES

1. Smith, D. E., F. J. Lerch, J. G. Marsh, C. A. Wagner, R. Kolenkiewicz, and W. D. Kahn, "Contributions to the National Geodetic Satellite Program by Goddard Space Flight Center," *J. Geophys. Res.*, **81** (5), February 1976, pp. 1006-1026.
2. Smylie, D. E., and L. Mansinha, "Earthquakes and the Observed Motion of the Rotation Pole," *J. Geophys. Res.*, **73** (24), December 1968, pp. 7661.
3. Smith, D. E., R. Kolenkiewicz, P. J. Dunn, H. H. Plotkin, and T. S. Johnson, "Polar Motion from Laser Tracking of Artificial Satellites," *Science*, **178**, October 1972, pp. 405-406.
4. Smith, D. E., R. Kolenkiewicz, and P. J. Dunn, "Earth Tidal Amplitude and Phase," *Nature*, **244**, August 1973, pp. 498-499.
5. Smith, D. E., and F. O. Vonbun, "The San Andreas Fault Experiment," *Acta Astronautica*, **1**, 1974, pp. 1445-1452.
6. Plotkin, H. H., T. S. Johnson, P. L. Spadin, and J. E. Moye, "Reflections of Ruby Laser Radiation From Explorer XXII," *Proceedings of the IEEE*, **53**, March 1965, pp. 301-302.
7. Marini, J. W., and C. W. Murray, "Correction of Laser Range Tracking Data for Atmospheric Refraction at Elevations Above 10 Degrees," NASA TM X-70555, 1973.
8. Zanter, D. L., C. S. Gardner, and N. N. Rao, "The Effects of Atmospheric Refraction on the Accuracy of Laser Ranging Systems," University of Illinois, RRL 481, January 1977.
9. Bar-David, I., "Communication Under the Poisson Regime," *IEEE Transactions on Information Theory*, **IT-15**, January 1969, pp. 31-37.
10. Lo, C. C., and Leskovar, B., "Evaluation of the Amperex 56TVP Photomultiplier," Lawrence Berkeley Laboratory, Report 5328, July 1976.
11. Abshire, J. B., "Systems for Measuring the Response Statistics of Gigahertz Bandwidth Photomultipliers," NASA TM-78029, November 1977.
12. Zagwodzki, T., "Testing and Evaluation of a State-of-the-Art Time Interval Unit," NASA TP-1051, September 1977.
13. Leskovar, B., and B. Turko, "Optical Timing Receiver for the Laser Ranging System, Part II: High Precision Time Interval Digitizer," Lawrence Berkeley Laboratory, Report 6133, February 1977.

14. Minott, P. O., "Design of Retrodirector Arrays for Laser Ranging of Satellites," NASA TM X-70657, March 1974.
15. Fitzmaurice, M. W., P. O. Minott, J. B. Abshire, and H. E. Rowe, "Prelaunch Testing of the Laser Geodynamic Satellite," NASA TP-1062, October 1977.
16. Agreen, R. W., and David E. Smith, "A Simulation of the San Andreas Fault Experiment," *J. Geophys. Res.*, **79** (29), October 1977, pp. 4413-4417.
17. Siry, J. W., "Crustal Motion Measurement by Means of Satellite Techniques," NASA TM X-70632, May 1973.
18. Fitzmaurice, M. W., P. O. Minott, and W. D. Kahn, "Development and Testing of a Spaceborne Laser Ranging System Engineering Model," NASA TM X-71037, November 1975.
19. Vonbun, F. O., W. D. Kahn, P. D. Argentiero, D. W. Koch, and K. J. Eng, "Spaceborne Earth Applications Ranging System," NASA TM X-71035, December 1975.

1. Report No. NASA TP-1149	2. Government Accession No.	3. Recipient's Catalog No.	
4. Title and Subtitle NASA Ground-Based and Space-Based Laser Ranging Systems		5. Report Date January 1978	
		6. Performing Organization Code 723	
7. Author(s) Michael W. Fitzmaurice		8. Performing Organization Report No. G7802-F03	
9. Performing Organization Name and Address Goddard Space Flight Center Greenbelt, Maryland 20771		10. Work Unit No. 506-18-26	
		11. Contract or Grant No.	
12. Sponsoring Agency Name and Address National Aeronautics and Space Administration Washington, D.C. 20546		13. Type of Report and Period Covered Technical Paper	
		14. Sponsoring Agency Code	
15. Supplementary Notes			
16. Abstract <p>Since the beginning of their development in the early 1960's, laser ranging systems have grown substantially within the National Aeronautics and Space Administration and have produced important precision-orbit and gravity-field determination results. Laser ranging is expected to help unlock the mysteries of the earthquake phenomenon by producing unique results of crustal motions of the Earth. The current state of the art and future projections are presented herein, including principal applications and characteristics of typical systems.</p>			
17. Key Words (Selected by Author(s)) Laser, Ranging		18. Distribution Statement STAR Category 35 Unclassified—Unlimited	
19. Security Classif. (of this report) Unclassified	20. Security Classif. (of this page) Unclassified	21. No. of Pages 28	22. Price* \$4.50

*For sale by the National Technical Information Service, Springfield, Virginia 22161.

National Aeronautics and
Space Administration

Washington, D.C.
20546

Official Business

Penalty for Private Use, \$300

THIRD-CLASS BULK RATE

Postage and Fees Paid
National Aeronautics and
Space Administration
NASA-451



NASA

POSTMASTER: If Undeliverable (Section 158
Postal Manual) Do Not Return
